Tribol Lett (2008) 29:85–94
DOI 10.1007/s11249-007-9285-y

ORIGINAL PAPER

Utilizing the Explicit Finite Element Method for Studying Granular Flows

M. A. Kabir · Michael R. Lovell · C. Fred Higgs III

Received: 25 June 2007 / Accepted: 29 November 2007 / Published online: 19 December 2007

Abstract Granular flows are systems of complex dry particulates whose behavior is difficult to predict during sliding contact. Existing computational tools used to simulate granular flows are particle dynamics, cellular automata (CA), and continuum modeling. In the present investigation, another numerical tool—the explicit finite element method (FEM)—is analyzed as a potential technique for simulating granular flow. For this purpose, explicit dynamic finite element models of parallel shear cells were developed. These models contained 52 particles and consisted of granules that are both round and multi-shaped (diamond, triangle, and rectangle). Each parallel shear cell consisted of a smooth stationary top wall and a rough bottom surface that was given a prescribed velocity of $U = 0.7$ in/sec (1.78 cm/s). The coefficient of friction (COF) between the particle–particle and particle–wall collisions was varied between 0.0 and 0.75. Utilizing the output of the simulations, results are presented for the shear behavior, particle kinetic energy, and particle stresses within the shear cell as a function of time. As a means of validating the explicit technique for granular flow, a 75 particle, zero roughness, couette shear cell model (solid fraction of 0.50) is subsequently presented for which direct comparisons are made to the results published by Lun. [Lun, C.K. et al.: Phys. Fluids **8**, 2868–2883 (1996)] Overall, the results indicate that the explicit FEM is a powerful tool for simulating granular flow phenomena in sliding contacts. In fact, the explicit method demonstrated several advantages over existing numerical techniques while providing equivalent accuracy to the molecular dynamics (MD) approach. These advantages included being able to monitor the collision (sub-surface and surface) stresses and kinetic energies of individual particles over time, the ability to analyze any particle shape, and the ability to capture force chains during granular flow.

Keywords Finite element method · Shear cell · Granular flow · Dry particulate lubrication

M. A. Kabir · M. R. Lovell · C. F. Higgs III
Pittsburgh Tribology Center, Pittsburgh, PA, USA

M. A. Kabir · C. F. Higgs III
Department of Mechanical Engineering, Carnegie Mellon University, 5000 Forbes Ave., Pittsburgh, PA 15213-3890, USA
e-mail: higgs@andrew.cmu.edu

M. A. Kabir · M. R. Lovell (✉)
School of Engineering, University of Pittsburgh, 323 Benedum Hall, Pittsburgh, PA 15260, USA
e-mail: mlovell@engr.pitt.edu

1 Introduction

Applications of granular flows can be found in both man-made processes and nature. In the industrial community, granular flows occur in chemical, metallurgical, ceramic, civil engineering, and pharmaceutical applications. In nature, examples of granular flow include avalanches, river sedimentation, dune formation, planetary ring dynamics, soil liquifaction, and ice flow mechanics.

Despite being somewhat commonplace, theoretically analyzing granular flow is difficult due to the complex motion and interaction of particles. For this reason, numerical tools are often used to study granular flow behavior. As observed in the literature, the most commonly used tool for simulating sheared granular flows are MD-type discrete element methods (DEM). When modeling atomistic-scale particles with perfectly elastic collisions, the approach is called MD. When modeling macro-scale

particles with inelastic collisions, the approach is usually called granular dynamics (GD), or more commonly, DEM. DEM can simulate particle motions/velocities and capture shearing effects in granular cells. Another approach recently introduced to the field of tribology to model granular flows is cellular automata (CA), which employs rule-based mathematics on a spatial lattice to simulate random shearing of granules. These tools are very powerful but have limited capabilities in simulating complex particle shapes, inhomogeneous granular materials, and the post-collision stresses and deformations of particles during flow. Granular flows sometimes behave like fluids; modified Navier–Stokes equations have been used to model them as a continuum, where the discrete granules are akin to dense fluid molecules [1–3]. Navier–Stokes equations can be solved easily for the simplest cases like water, and when they are modified for use with granular flows, they become increasingly more complex.

Originally proposed as an alternative form of lubrication for high-temperature tribomachinery, granular flows have been studied in tribology. However, the complex interactions of granular media make the problem rich for tribological studies, as evidenced by the multiple modes of tribo-physics that exist. For example, granular flows are comprised of numerous frictional interactions [4, 5], contact mechanics [6, 7], and lubrication characteristics [1, 2, 8–10]. Wornyoh et al. recently conducted a review of granular flows in the field of tribology that occurred in annular, bearing-type, and parallel shear cell geometries. [11]. Although not considered a practical industrial application, parallel shear cells are used to conduct fundamental theoretical studies of many types of granular flows. This shear cell geometry remains a robust configuration for exploring newly developed theoretical and computational modeling approaches, and for establishing benchmarks for comparing various models. For example, Sawyer and Tichy used the parallel shear cell to compare a granular continuum model to a DEM model of the same granular materials [2]. Higgs and Tichy later developed a more robust granular kinetic lubrication (GKL) continuum model of granular flows to study granular materials in a parallel shear cell and compared the modeling results to those from actual granular shear cell experiments [1]. Jasti and Higgs introduced the lattice-based CA modeling approach to the field of tribology as a tool for employing rule-based mathematics to study granular flows [12]. They compared their new CA model to the GKL continuum model for granular flows in a parallel shear cell. Others have also introduced new granular flow models and studied various characteristics of granular flows in parallel shear cells [13–16]. Additional studies have been conducted using a molecular dynamics (MD) approach to study a steady-state, gravity-free Couette flow of inelastic hard spheres with rough walls [15, 16]. In these works, numerical programs were developed to simulate rapid granular flow in a Couette shear cell geometry.

This article introduces the explicit finite element method (FEM) as a powerful numerical tool to study granular flows. The granular materials studied in this work were sheared between two parallel walls with one translating rough surface, no gravity, and no externally applied load. More specifically, the present work demonstrates that shearing effects, post-collision stresses, deformation and kinetic energy histories of granular particles can be captured using explicit FEM. Such information is essential for predicting flow behavior such as the onset of GKL, where the granular flow particles change from slowly shearing materials to rapidly colliding materials. A dilute (mean solid fraction $v_o = 0.55$) granular flow of 52 particles with roughness along the bottom surface is introduced to simulate round and multi-shaped (i.e., round, diamond, triangle, and rectangle) particles. The mean solid fraction is the percentage of the shear cell area (in 2D) or volume (in 3D) that is comprised of solid granular particles. Since the shear cell in this work is two-dimensional, the mean solid fraction is an areal fraction. Different friction coefficients are applied within the cell to investigate their role on the particle flow behavior and the magnitude of the post-collision stresses. As a means of validating the explicit technique for granular flow, a 75 particle, zero roughness, couette shear cell model (solid fraction of 0.50) is subsequently presented for which direct comparisons are made to MD results published by Lun [16].

2 Explicit Finite Element Method Time Integration

With the tremendous advances in computational resources over the last decade, the number of numerical techniques available to engineers and scientists has grown enormously. One of these techniques, the FEM has become widely used in the tribology community to study complex contact, thermal, fluid, and structural interaction. In the finite element analysis arena, two distinct methods, the implicit and explicit time integration techniques, have emerged for simulating engineering and scientific problems. Although both of these methods are used to solve the same basic set of governing equations, the primary applications for which each method obtains a robust accurate solution are vastly different. Explicit FEMs were originally developed to solve problems in wave propagation and impact engineering, but they have been more recently applied to diverse areas that include sheet metal forming, underwater simulations, failure analyses, glass forming, metal cutting, pavement design, and earthquake engineering [17].

In the implicit FEM, commonly referred to as the standard Newmark method, a forward difference technique is applied with constant average accelerations. The general governing equations of the implicit method for structural problems are evaluated at time t_{n+1} [18]. For the case of explicit finite element time integration, the central difference method is applied and a linear change in displacements is assumed [19]. Therefore, unlike the implicit method, the general governing equations are evaluated at time t_n:

$$[M]\{\ddot{u}_n\} + [C]\{\dot{u}_n\} + [K]\{u_n\} = \{F_n^a\} \tag{1}$$

and the expressions for the nodal accelerations and velocities are given by:

$$\ddot{u}_n = \frac{1}{\Delta t^2}(u_{n+1} - 2u_n + u_{n-1}) \tag{2}$$

and

$$\dot{u}_n = \frac{1}{2\Delta t}(u_{n+1} - u_{n-1}) \tag{3}$$

Substituting (3) and (2) into (1) we obtain an expression to solve for the unknown displacements $\{u_{n+1}\}$:

No difficulty for nonlinear problems

$$\left(\frac{1}{\Delta t^2}[M] + \frac{2}{\Delta t}[C]\right)\{u_{n+1}\} = \{F_n^a\} - \left([K] - \frac{2}{\Delta t^2}[M]\right)\{u_n\} - \left\{\frac{1}{\Delta t^2}[M] - \frac{1}{2\Delta t}[C]\right\}\{u_{n+1}\} \tag{4}$$

In the explicit method, the matrix $[M]$ is a lumped (diagonalized) mass matrix and $[C]$ is a mass proportional damping matrix created from $[M]$. For this case, we find that the system of Eq. (4) become uncoupled so that each equation may be solved for explicitly. For nonlinear problems, the explicit method therefore requires significantly less memory and analysis time per iteration when compared to the implicit method, which must iterate to obtain a solution. Furthermore, it can be observed in Eq. (4) that the stiffness matrix $[K]$ is not required to be inverted to solve for the displacements, causing the solution procedure to be very stable for nonlinear problems. The primary drawback of the explicit technique relates to the fact that a critical time step is required to attain accurate results [20].

3 Explicit Finite Element Modeling of a 2D Granular Shear Cell

Utilizing the commercial explicit finite element analysis code ANSYS/LS-DYNA, gravity-free granular 2-D shear cells with 52 round (Fig. 1a) and multi-shape (Fig. 1b) particles were created with a roughness of $R = 1$ along the bottom cell surface. The roughness factor R varies between 0 and 1, where $R = 0$ corresponds to a smooth surface, and $R = 1$ represents a very rough surface where the slip is minimum. While the literature has interpreted the roughness factor R in several ways, the authors employ the definition of R as the fraction of granule that fits in the gap between the wall disk "asperities" [12]. This definition is straightforward to implement in simulations, as shown in Fig. 2. The overall dimensions of the round and multi-shape shear cells were 12 in (30.48 cm) long and 1.7 in (4.32 cm) high. In the shear cell with round particles, each particle had an

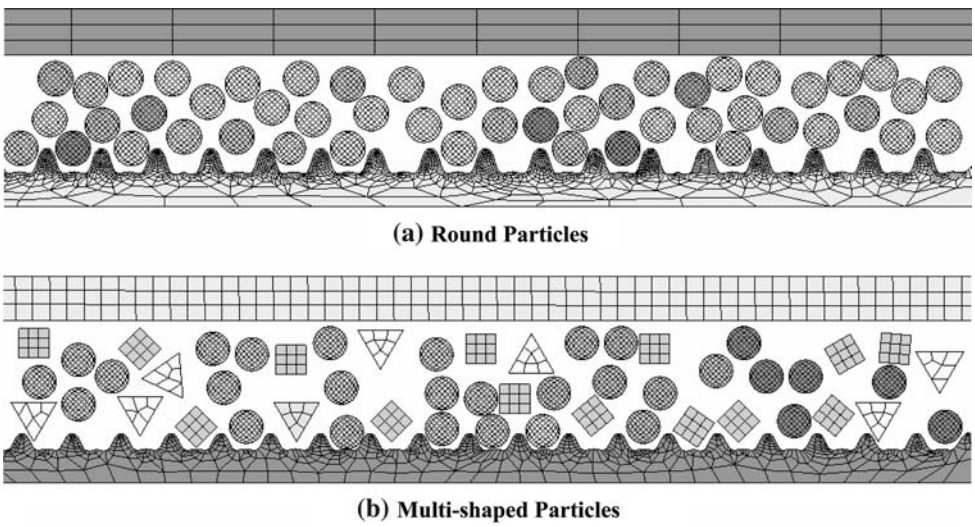

Fig. 1 2-D 52 Particle Granular flow shear cell finite element model

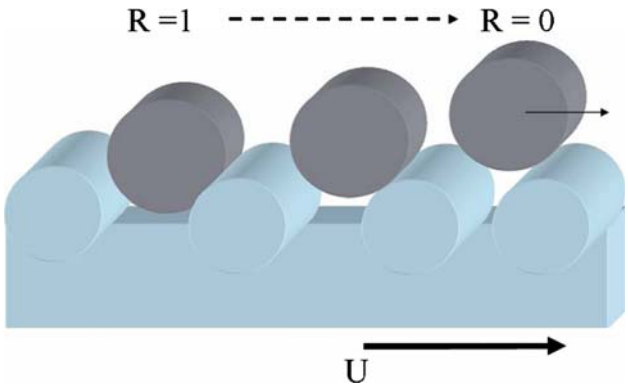

Fig. 2 Schematic of roughness factors

area of 0.07 in^2 (0.45 cm^2). Likewise, in the multi-shaped particle cell, the round, diamond, rectangle and triangle shapes were defined with a constant area of 0.07 in^2 (0.45 cm^2). The top and bottom surfaces of the cell, as well as the particles, were meshed with standard structural solid elements. Both the round and multi-shaped particle shear cells were randomly distributed within the cell and simulated for a mean solid fraction $v_o = 0.55$. The total number of elements in the 52 round shape particles shear cell was 6,249, as the number of elements in each particle was 64. The total number of elements in multi-shape particle shear cell was 3,450; the multi-shaped particle cell had a lower number of elements because the triangular and diamond shaped particles consisted of 6–7 and 9 elements respectively.

The shear cell consists of a couette-driven parallel configuration where the top surface is smooth and stationary while the bottom surface is rough and moving. Similar to slider bearings in tribology that represent an unwrapped journal bearing with a converging gap, the parallel shear cell is analogous to unwrapped concentric cylinders. In the finite element model, the walls and particles in the shear cell model were considered elastic steel; therefore, an elastic material model was defined for all of the components within the model (see Table 1). In addition, the entire finite element mesh consisted of Plane 162 elements and a single surface contact (ASS2D) was used to define all of the contact between the components within the model.

A coulomb friction model was used in all simulations and the coefficients of friction (COF) were varied between $\mu = (0, 0.25$ and $0.75)$ to study the friction's influence on the granular flow. The COF defined the friction in both particle to particle and particle to wall contact. A COF equal to 0 represents a smooth surface or frictionless environmental in the shear cell and was studied strictly for academic purposes. The boundary and loading conditions applied in all the finite element simulations were as follows. The upper wall of the shear cell was held stationary ($U = 0$) while the bottom wall was given a constant velocity of $U = 0.7$ in/sec (1.78 cm/s). Initial velocities of 0.7 in/sec (1.78 cm/s) were applied to 16 particles of each shear cell to induce collision among particles and walls. These velocities were chosen arbitrarily to energize the flow since the gravity-free condition minimizes the amount of uniformly dispersed particles engaged in collisions within a simulation.

Table 1 Material model parameters

Density lb/in^3 (kg/m^3)	0.284 (7,850)
Young's modulus lbf/in^2 (Pa)	30×10^6 (210×10^9)
Poisson's ratio	0.294
Mean solid fraction	0.55

4 Results and Discussions

4.1 Shearing Effect, Force Chains, and Particle Shapes

The primary goal of the present investigation is to establish whether the explicit FEM can be used to study granular flow behavior. Examining the results, it is apparent that explicit FEM is able to replicate particle motion within a simple shear cell, particularly with respect to shearing effects, particle collisions, and kinetic energy behavior. As described in prior work by the authors [1, 12], the moving rough bottom wall surface of a shear cell is the primary energy source for inducing granular flow motion and shearing. In our explicit finite element simulations, the moving bottom wall clearly produced classical granular flow and shearing effects for both round and multiple shaped particles. The simulations consist of 52 particles, which are enough to study granular flow in shear cells, but not enough to meet a criterion for being a granular flow continuum [1], which would be more computationally expensive. As indicated by the particle stresses in Fig. 3a,b for the geometrically homogenous and inhomogeneous granular flow respectively, the moving bottom wall induced collisions among particles and the walls during motion. As expected, it was observed that discrete particles close to the bottom wall moved at the highest velocity in the direction of shear and the particles near the top wall had little motion.

Using explicit FEM, Fig. 4 was generated to illustrate the variation of granular velocity across the height of the shear cell for both round ($\mu = 0, 0.25$, and 0.75) and multi-shaped ($\mu = 0.25$) particles. In Fig. 4, the particle conditions examined exhibited similar nonlinear yet couette-flow type velocity trends. The main difference from conventional fluids is that granular flows slip at the boundaries, which means that the flow's velocity is not the same as the top and bottom walls (i.e., $u/U = 0$ and 1, respectively).

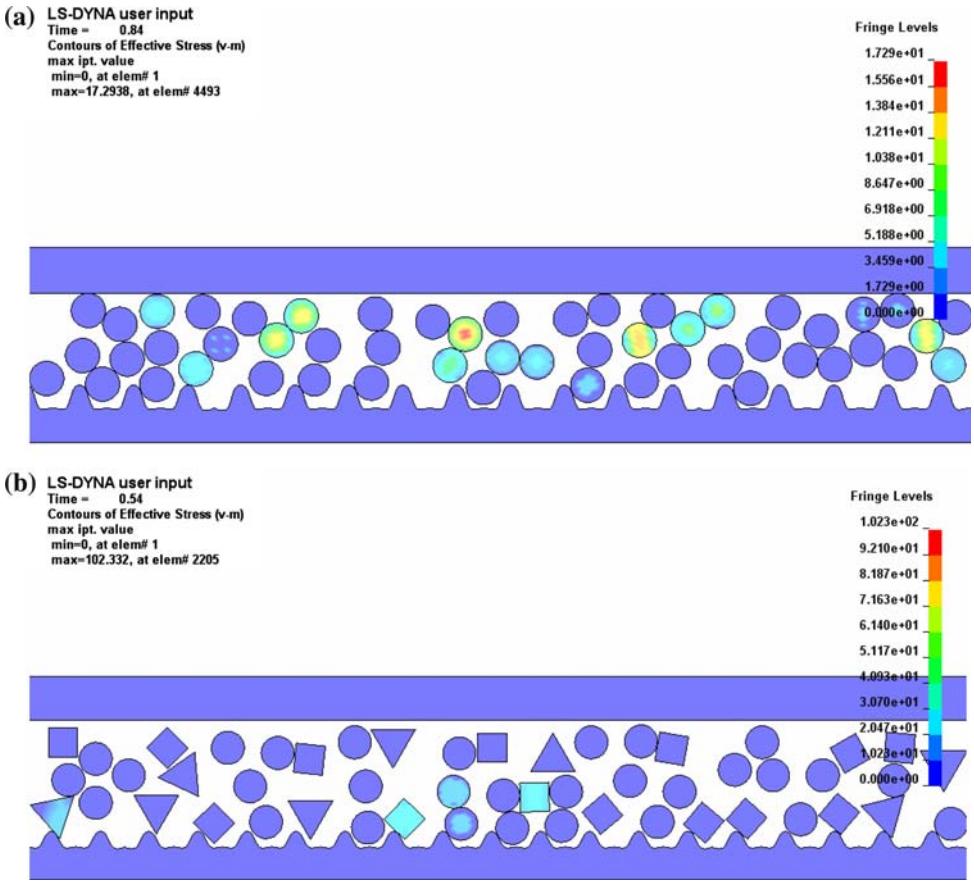

Fig. 3 (**a**) Contact stresses within 52 round particle simulated shear cell, (**b**) Contact Stresses within 52 particle multi-shaped shear cell

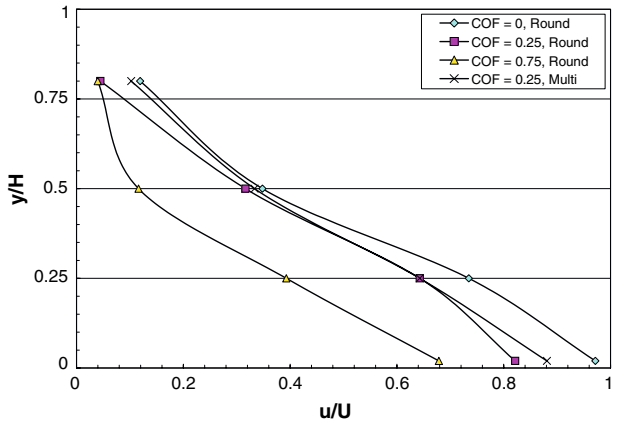

Fig. 4 Granular flow velocity across height of shear cell

The linearly decreasing velocity trend across the gap was also observed in the computational and theoretical analyses of granular flows using CA [12] and GKL [1], respectively.

Another trend observed in Fig. 4 is that the granular flow comprised of round particles exhibit an inverse relationship between velocity and friction coefficient in the region near (i.e., $y/H < 0.2$) the moving wall. This is because the energy being imparted to the flow by the moving wall is dissipated by the friction. Therefore, a lower friction coefficient enables more energy to be available to move the granules in the direction of the moving wall. One non-intuitive trend is that the granular flow comprised of multi-shaped particles ($\mu = 0.25$) appeared to have more energy and a higher velocity near the moving wall, than the round particles with the same imposed friction coefficient. This perhaps can be explained from contact mechanics, where the maximum contact pressure P_{max} in Eq. (5a) between the two particle geometries (i.e., round/round, round/square, and round/triangular) colliding at the same speed can be compared. Since the effective radius of curvature R for round/round contact is greater than R for round/square and round/triangle contact, the contact pressure for round/round collisions (see Fig. 3a) would be higher than that for round/square and round/triangle collisions (see Fig. 3b). This can be seen in the Hertzian contact formulas in Eq. (5b), where F_n is the force due to collision, E' is the composite elastic modulus between the colliding particles, and R_a and R_b are the radii of curvature for the first and second colliding particle. Assuming that the round/triangle and round/square particles collide on one of the triangle or square sides, R will be larger for the multi-shaped particle collisions.

Therefore, it is more likely that plastic deformation is induced in the round/round collisions since they have higher contact pressures (for the same collision force F_n), which means the rebound velocities (and hence granular flow velocity) for round particle granular flows will be lower due to the inelastic collisions.

$$P_{\max} = \frac{1}{\pi}\left(\frac{6F_n E'^2}{R^2}\right)^{1/3} \tag{5a}$$

$$\frac{1}{R} = \frac{1}{R_a} + \frac{1}{R_b} \tag{5b}$$

An additional result of the 52 particle simulations is the appearance shear force chains among the particles. These force chains, which have been found experimentally [21], are another important indication that our explicit FEM approach can be used to capture complex granular flow behavior. As shown in Fig. 5, collisions took place among and between the particles and the shear cell wall. These collisions led to visible stresses and deformations within the particles of the cell. Closely examining Fig. 5, a 'force-chain' clearly developed between the particles across the height (top wall to bottom wall) of the cell. This chain looks similar to the results of existing experimental techniques [21] that captured the force-chains in dense granular medium. Such as finding is important since albeit is difficult to successfully predict force-chains, and the particle stresses and deformations in granular flows.

A final important finding of the finite element results presented in Figs. 3b and 4 are that the explicit FEM is capable of simulating granular flow for particles of any geometry. In fact, Fig. 4 distinctly indicates that the velocity profile across the shear cell ($\mu = 0.25$) distinctly varies between the round and multiple particle shape cases. Therefore, the FEM framework is well-suited for simulating aspherical or multi-shaped particles.

4.2 Particle Stresses and Energy History

Another goal of the present investigation was to determine the effectiveness of the explicit FEM for analyzing the post-collision stresses and deformations of particles within a shear cell. In the previous section, the explicit FEM based tool predicted post-collision stresses and deformations (see Figs. 3a,b and 5) among particles in the granular flow shear cell of different shaped particles. In these figures, the von Mises stresses are captured at specific points in time. In this section, we hope to demonstrate that the instantaneous post-collision behavior of any particle within the cell can be captured in detail. For this purpose, the authors investigated the von Mises stresses of specific particles in a frictionless ($\mu = 0.0$) shear cell just before ($t = 0.24$ s) and after ($t = 0.25$ s) they impacted. In Fig. 6a, the two round particles of interest (i.e., particles 1 and 2) do not show any stress contours before they collide. Just after the collision, at time = 0.25 s, the stress contours in Fig. 6b clearly indicate that significant stress has developed within the particles. Such a finding indicates that explicit FEM provides more detailed information on particle behavior than conventional particle dynamics approaches.

To further explore the capability of explicit FEM for simulating granular flows, we will examine the stress behavior of a specific particle over an entire simulation period (5 s). The specific particle of interest, shown in Fig. 7, is part of a round particle shear cell analysis in the absence of friction. During the simulation, the maximum

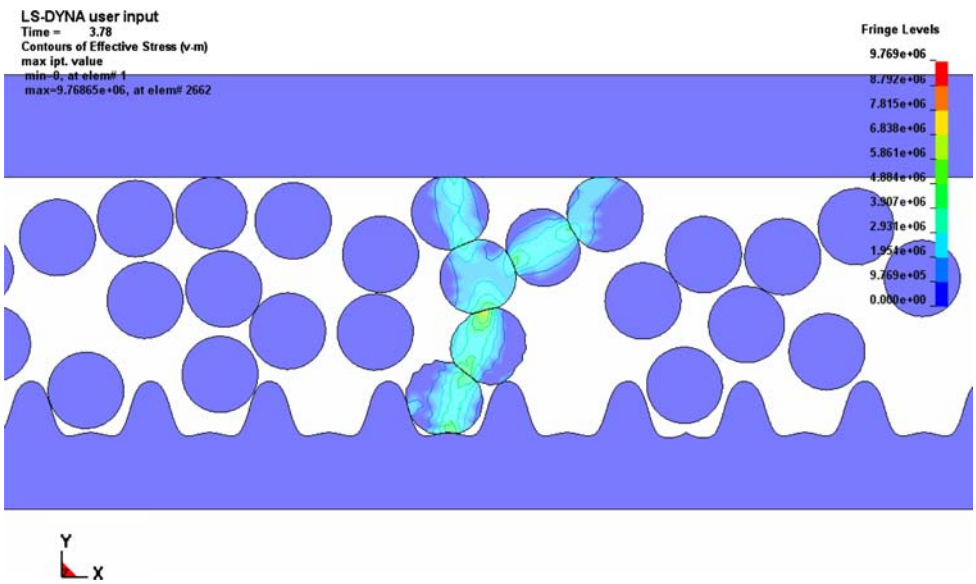

Fig. 5 Stress, deformation and force-chain in 52 particles shear cell

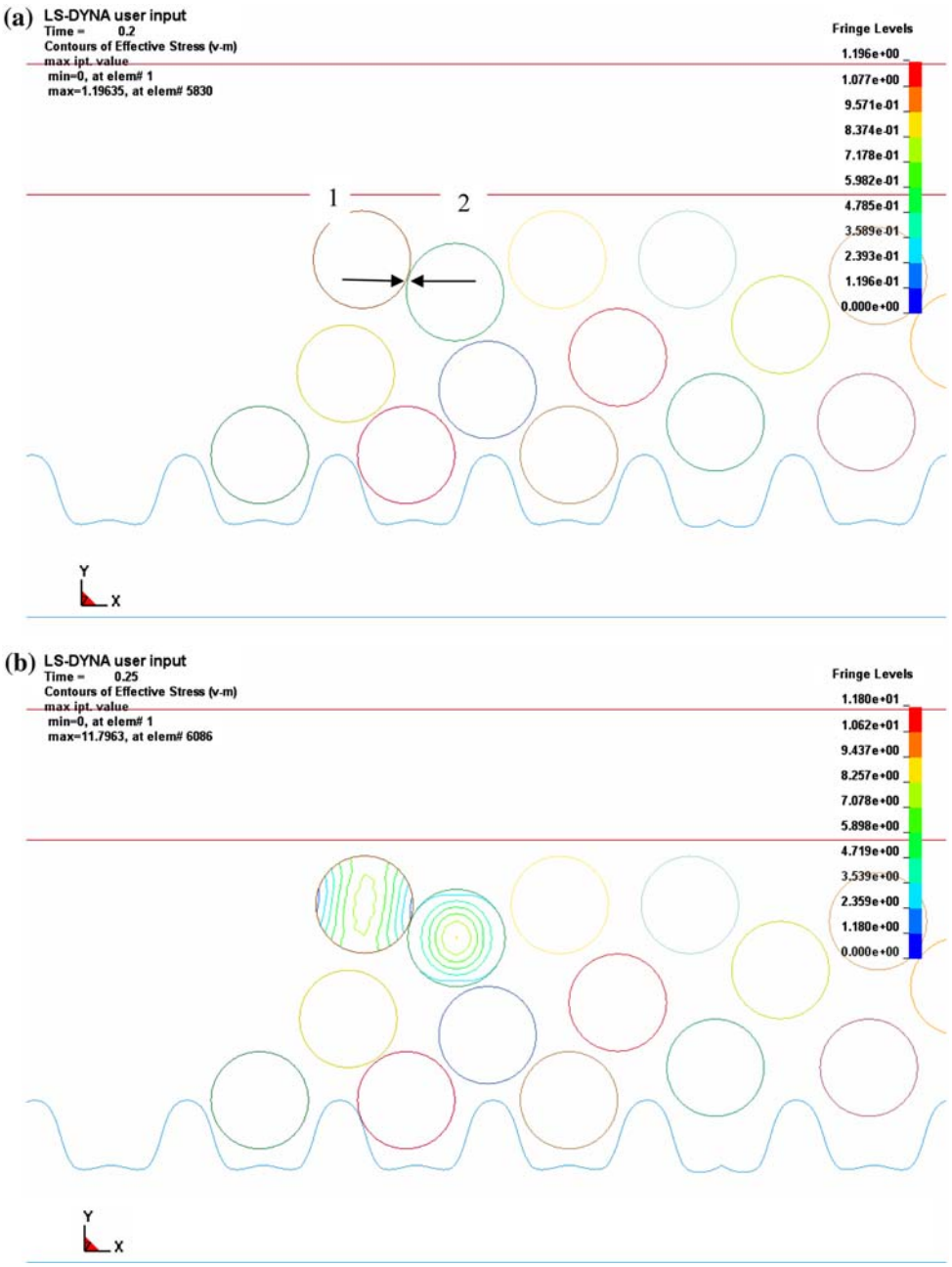

Fig. 6 (**a**) Particles *just before* first collision at $\mu = 0$ in round particles shear cell, (**b**) Particles *just after* first collision at $\mu = 0$ in round 52 particle shear cell

stress history of the particle was monitored and plotted as a function of time. As shown in Fig. 8, the explicit FEM simulation was able to capture the collision and stress history of the particle. In the simulated results, it is found that the first particle collision took place 1.05 s and the elements von Mises stress increased to 10 psi (68.9 kPa). Moving forward in time, the particle then releases stress until a second more pronounced collision took place near 3 s when the particle contacted the moving bottom wall. At this instance in time, the element attained its maximum stress level of 70 psi (482.6 kPa) stress. Throughout the remainder of the simulation, two other particle collisions are found to take place near 4 and 5 s where the stresses attain values of 7 psi (48.2 kPa) and 5 psi (34.5 kPa), respectively. By analyzing the chronology of a specific particle, one can determine practical parameters such as the criterion for cracking of round fruit being transported on a moving conveyor system. Food industries that may want to reduce abrasions, dents, and punctures on fruit during processing can be provided with a set of conditions for a yielding more undamaged fruit.

When analyzing granular flow, the kinetic energy history of both the entire shear cell and the individual particles are often of interest. As illustrated in Fig. 9, the

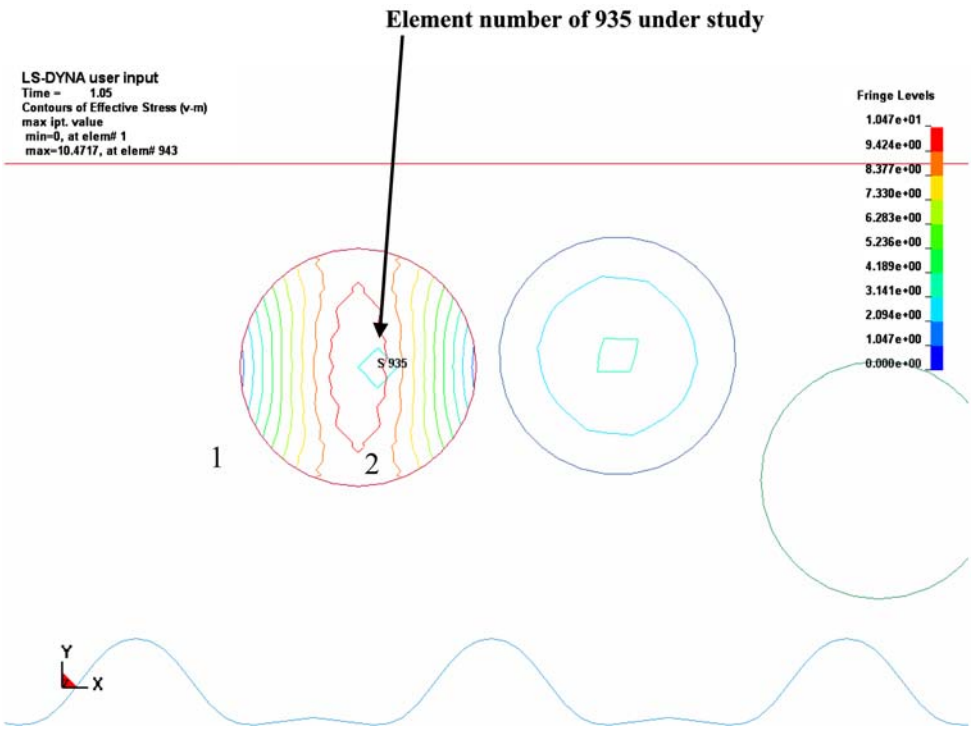

Fig. 7 This figure shows the element of interest (#935) of a frictionless particle

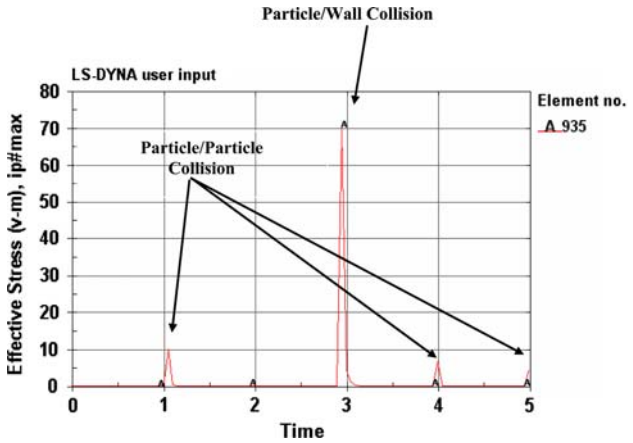

Fig. 8 The stress history for element of interest (#935)

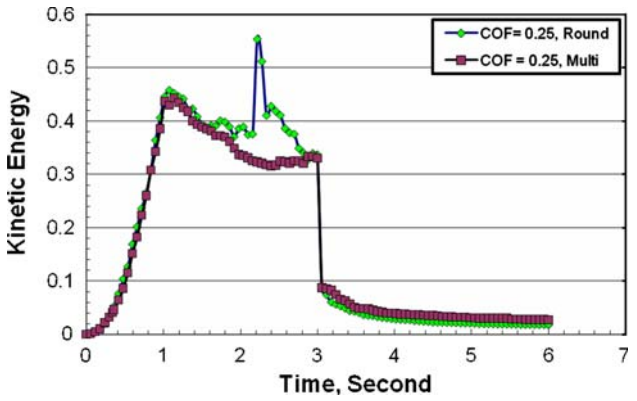

Fig. 9 Shows the global kinetic energy history of 52 particles shear granular shear cell

overall kinetic energy of the entire cell can be captured as a function of time using the explicit FEM. The results in Fig. 9 represent the kinetic energy history of the cell for different shaped particles (with identical areas) experiencing the loading conditions described in Sect. 3. Likewise, Fig. 10 shows the kinetic energy history of the individual particle from Fig. 7 at friction coefficients values of 0, 0.25, 0.50, and 0.75. As illustrated in Fig. 10, the dynamics of the particle of interest is clearly captured in the simulations. The particle remains stationary until it was hit by another particle at around $t = 1$ s. The particle then moves and has an increase in kinetic energy before slowing and making contact with another particle. An interesting result of Fig. 10 is that the kinetic energy and collision history of the particles significantly fluctuate with friction coefficient. Being able to monitor both local and global kinetic energy histories is important as it allows one to conclude whether the granular shear cell has thermodynamically reached a steady-state condition.

4.3 Validation of Explicit Technique

As discussed in the previous sections, the explicit FEM offers several distinct advantages over traditional

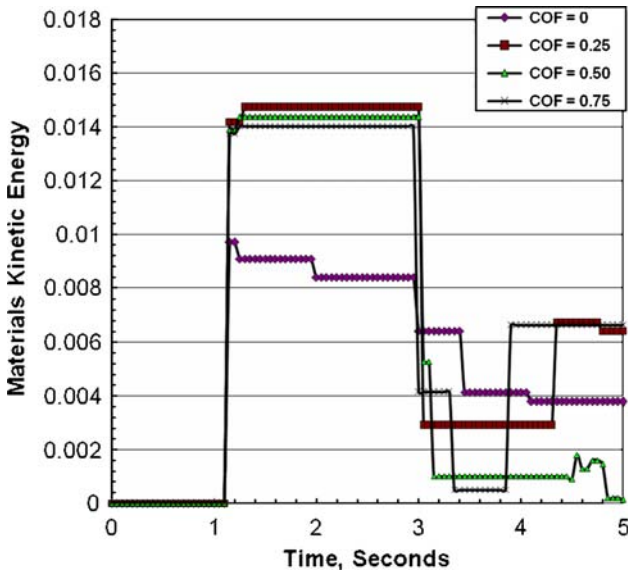

Fig. 10 Kinetic energy over time at different friction coefficients

approaches for modeling granular flow. Without validation, however, the actual results predicted by the method will hold little value to the scientific community. For this purpose, a 72 particle explicit dynamic finite element shear cell model (see Fig. 11a) was constructed with identical geometry, material, and shearing conditions to the shear cell presented by Lun [16]. In his work, Lun performed MD simulations for a gravity-free shear cell with round steel particles and a smooth wall (i.e., roughness factor $R = 0$). In Lun's cell, the gap height (H) between the two rough parallel plates was $5d$, where d is the particle diameter. Roughness along the walls was defined using hemispherical particles that were attached to the wall surfaces and a particle solid friction of 0.50 was studied. Following the work of Lun, FEM simulations were performed using the geometry shown in Fig. 11a by holding the bottom plate stationary while the top plate was moved at a constant velocity of U. In the simulations, a friction coefficient of 0.35 was defined for both particle to particle and particle to wall contacts. To determine the accuracy of the explicit finite element approach, the predicted velocity and solid fraction profiles across the height of the shear cell were compared for the FEM and Lun's published MD simulations. As graphically illustrated in Fig. 11a,b, the finite element and MDs simulations predicted nearly identical results for both the velocity and solid fraction profiles. Such a finding is extremely important because it indicates that the explicit FEM not only provides additional information (such as particle stresses) to better understand granular flow, but its accuracy is on the same order of magnitude as MDs simulations for predicting granular flows.

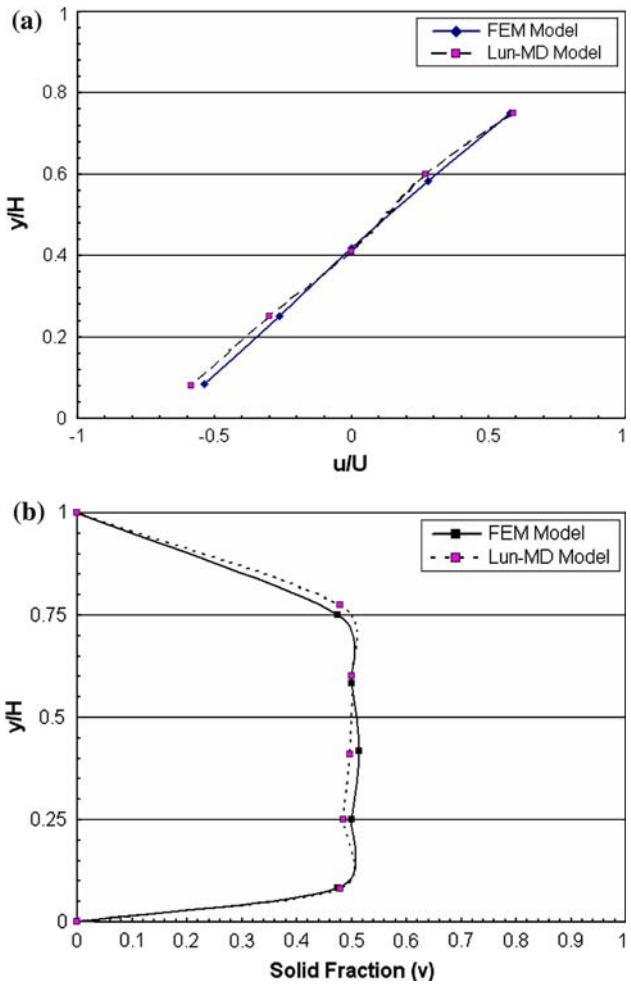

Fig. 11 (**a**) Velocity comparison across height of Lun-MD and FEM models, (**b**) Solid fraction comparison of Lun-MD and FEM models

5 Conclusions

This article investigates the possible use of the explicit FEM as numerical tool for analyzing granular flow behavior. For this purpose, finite element models of granular shear cells with only 52 particles were developed to simulate the dynamics of round and multi-shaped (round, diamond, triangle, and rectangle) particles. In the shear cell, a moving bottom wall was given a rough surface, and different friction coefficients were applied to analyze particle flow behavior and the magnitude of the post-collision stresses. Based on the numerical results, the explicit FEM showed significant promise for use in full-scale granular flow problems. In fact, the explicit method demonstrated key factors advantageous for modeling complex granular flows. These advantages included being able to monitor the collision stresses and kinetic energies of individual particles over time, the ability to seamlessly analyze any particle shape, and the ability to capture force chains

during granular flow. Furthermore, by comparison to published work [16], the method was found to be on the same order of accuracy as the molecular dynamics method for predicting particle flow behavior.

Acknowledgments The authors would like to thank the Mascaro Sustainability Initiative (MSI) and the members of the Pittsburgh Tribology Center, a collaboration between the University of Pittsburgh and Carnegie Mellon University.

References

1. Higgs, C.F., Tichy, J.: Granular flow lubrication: continuum modeling of shear behavior. Trans. ASME J. Tribol. **126**, 499–510 (2004)
2. Sawyer, W.G., Tichy, J.: Lubrication with granular flow: continuum theory, particle simulations, comparison with experiment. Trans. ASME J. Tribol. **1234**, 777–784 (2001)
3. Hui, K. et al.: Boundary conditions for high shear grain flows. J. Fluid Mech. **145**, 223–233 (1984)
4. Thompson, P.A., Grest, G.S.: Granular flow: friction and the dilatancy transition. Phys. Rev. Lett. **6713**, 1751–1754 (1991)
5. Pouliquen, O., Forterre, Y.: Friction law for dense granular flows: application to the motion of a mass down a rough inclined plane. J. Fluid Mech. **453**, 133–151 (2002)
6. Jang, J.Y., Khonsari, M.M.: On the role of enduring contact in powder lubrication. J. Tribol-T. ASME **1281**, 168–175 (2006)
7. Savage, S.B., Jeffrey, D.J.: The stress tensor in a granular flow at high shear rates. J. Fluid Mech. Digital Archive **110**, 255–272 (2006)
8. Yu C., Craig K., Tichy J.A.: Granular collision lubrication. J. Rheol. **38**(4):921–936, (1994)
9. Jang, J.Y., Khonsari, M.M.: On the granular lubrication theory. Proc. Royal Soc. A Math Phys. Eng. Sci. **4612062**, 3255–3278 (2005)
10. Iordanoff, I., Khonsari, M.M.: Granular lubrication: toward an understanding of the transition between kinetic and quasi-fluid regime. J. Tribol. **1261**, 137–145 (2004)
11. Wornyoh, E.Y.A., Jasti, V.K., Higgs, C.F. III: A review of dry particulate lubrication: powder and granular materials. J. Tribol. **129**, 438 (2007)
12. Jasti V.J., Higgs III C.F.: A lattice-based cellular automata modeling approach for granular flow lubrication. Trans. ASME J. Tribol. **128** (2):358–364 (2006)
13. Yu C., Tichy J.A.: Granular collision lubrication: effect of surface roughness, particle size, solid fraction. STLE Tribol. Trans. **39**, 537–546 (1996)
14. Zhou, L., Khonsari, M.M.: Flow characteristics of a powder lubricant sheared between parallel plates. J. Tribol. **122**, 147–154 (2000)
15. Louge, M.Y., Jenkins, J., Hopkins, M.A.: Computer simulations of rapid granular shear flows between parallel bumpy boundaries. Phy. Fluids A **2**, 1042 (1990)
16. Lun, C.K. et al.: Granular dynamics of inelastic spheres in Couette flow. Phys. Fluids **8**, 2868–2883 (1996)
17. Tavárez, F.A.: Simulation of behavior of composite grid reinforced concrete beams using explicit finite element methods. UNIVERSITY OF WISCONSIN—MADISON: MADISON (2001)
18. Hughes, T.: The Finite Element Method: Linear Static and Dynamic Finite Element Analysis. Courier Dover Publications (2000)
19. Huebner, K.H.: The Finite Element Method for Engineers. Wiley-IEEE Publishers (2001)
20. Smith I.M., Griffiths D.V.: Programming the Finite Element Method. Wiley, New York (2004)
21. Majmudar, T.S., Behringer, R.P.: Contact force measurements and stress-induced anisotropy in granular materials. Nature **435**, 1079–1082 (2005)